SUPPLEMENTAL INFORMATION TO MANUSCRIPT

Interpolation Method

The temperature interpolation method used in this study involved three steps. The first step was to fill in missing values using data from nearby stations that have good correlation. Temperature data was strongly correlated ($r > 0.9$) at distances up to 1000 km between stations, similar to findings in networks of rainfall and temperature stations in Peru and Switzerland [55]. However, temperature interpolation was limited to stations within 100 km of each other to limit the deviation in mean temperature between stations, and stations with $r > 0.9$ were used to interpolate missing values. This interpolation produced 68 temperature time series with greater than 95% completion (i.e., less than 5% of the time series had missing data) of which 61 had >99% completion. In a second round of interpolation, the remaining missing values were replaced using the average of the 2 measurements from the same month in the years before or after the missing value. Lastly, any remaining missing values were linearly interpolated from the first point before the missing value to the first point after the missing value.

This interpolation method can be summarized as follows: gaps in time series are first filled in with the nearest and most highly correlated rainfall stations, followed by using the average of the preceding or proceeding 2 years for a given month if any missing values remained, and lastly using linear interpolation to resolve any remaining gaps after the second step. Temperature time series were then assigned to each drainage basin based on proximity to the centroid of the basin. 50 of the 68 basins in this study had multiple NOAA stations (of the 69 stations used in this study) within 50 km of its centroid. After the time series from the NOAA station nearest each basins' centroid was

assigned to each basin, other stations' time series were used to extend each basins' assigned time series. This extension simply appended any data existing beyond the initial time series' first or final date before or after the start or end of the initial time series. Time series extension was necessary to increase the time series' length beyond 80 years (one AMO cycle) as 19 of the 69 NOAA stations had less than 80 years of recorded data. Fourteen of the 68 basins had only one NOAA station within 50 km of its centroid and these basins' time series thus were not extended. Four of the 68 basins did not have a NOAA station within 50 km (the greatest distance was 77 km) because either the basin was too small or the local spatial resolution of stations with long records was low. Thus, only the NOAA station nearest these 4 basins' centroids was used for the temperature time series.

Basin Delineation

The delineation method using the USGS Water Boundary Dataset (WBD) (used for 11 basins) sometimes needed approximation if a gaging station was inside a delineated drainage area rather than at its boundary. One basin was delineated using both the WBD and data from SWFWMD. Three basins were delineated by South Florida Water Management District (SFWMD). Two basins were springsheds and were delineated using flow nets and potentiometric surface maps by the Florida Department of Environmental Protection (FDEP). Lastly, two basins were delineated manually in QGIS with GRASS tools and digital elevations from the Shuttle Radar Topography Mission (SRTM) by the National Aeronautics and Space Administration (NASA). Each delineated basin was converted into the NAD83 / Florida GDL Albers projection.

Detailed Methodology Work-Through

The purpose of this section is to provide readers more details on the methodology by working through two of the 68 basins analyzed in this study. One basin was determined to have significant

evidence of FSI impacts to the water mass balance (Basin 48, Silver Springs, FL). Another basin was determined as unlikely to be impacted by the FSI (Basin 46, Satilla River, GA). These two basins were evaluated for FSI impacts by estimating long term time lag (Δt) between R and Q_b and by estimating the storage coefficient (S) for each basin. Basins satisfying the following two conditions were considered to have evidence of FSI impacts to the water balance: 1) mean Δt > 1 year with coefficient of variation < 0.3, and 2) S > porosity (η). The maximum value for η was discussed in the main text as 0.4.

Table S1: Statistics showing the quantity of missing values and the percentage of groundwater contribution to streamflow in the two basins.

Basin	Stream Flow Data % Completeness	% GW
Basin 46 – Satilla River, GA	100.0	55.0
Basin 48 – Silver River, FL	100.0	97.0

Water Balance

First, baseflow (Q_b) was separated from streamflow using the methodology recommended by Nathan and McMahon [32] with filter parameter equal to 0.925. Missing values, which weren't present in these 2 basins (Table S1), were linearly interpolated prior to baseflow separation. Average groundwater contribution to streamflow (Q_s) was determined by taking the mean value of the baseflow time series divided by the streamflow time series:

$$\% \, GW = 100 * \left(\frac{Q_b}{Q_s}\right)_{mean}$$

Time series of monthly precipitation (P) were downloaded from PRISM [33] for the period 1895-present at the centroid of each basin. Next, evapotranspiration (ET) was estimated using temperature data from NOAA. These temperature datasets were interpolated using the methodology

described at the beginning of this Supplemental Information document. Potential ET (PET) was estimated using the Turc equation assuming relative humidity > 50% from Lu et al. [34]

$$PET = 0.013\left(\frac{T_m}{T_m + 15}\right)(R_s + 50)$$

where T_m is daily mean air temperature and R_s is daily solar radiation estimated from Hargreaves and Samani [35]

$$R_s = k_{RS} R_a (T_{max} - T_{min})^{0.5}$$

where T_{max} is daily maximum temperature, T_{min} is daily minimum temperature, k_{RS} is the empirical radiation coefficient, and R_a is daily extraterrestrial radiation. The empirical radiation coefficient was estimated from Samani [36] who used 65 weather stations in the United States to determine the relationship between k_{RS} and $(T_{max} - T_{min})$ with $R^2 = 0.70$,

$$k_{RS} = 0.00185(T_{max} - T_{min})^2 - 0.0433(T_{max} - T_{min}) + 0.4023$$

Daily extraterrestrial radiation was estimated from Allen et al. [37] under the radiation section of chapter 3 which outlines the procedure for estimating R_a using the global solar constant, inverse relative Earth-Sun distance, sunset hour angle, latitude, and solar decimation.

After converting PET from daily resolution to monthly resolution, ET was then estimated using the Choudhury [38] equation with the landscape parameter set to the default value of 1.8

$$ET = \frac{P}{\left(1 + \left({}^{P}/_{PET}\right)^{\alpha}\right)^{1/\alpha}}$$

where α is the landscape parameter.

Next, groundwater pumping (Q_p) time series were created for each basin by scaling state-level groundwater pumping data (Q_{state}) from USGS to the watershed scale using fractional areas

$$Q_p = Q_{state}\frac{A_{basin}}{A_{state}}$$

where A_{basin} is the drainage basin area and A_{state} is the area of the state that the basin is in. The state-level groundwater data were estimated every 5 years by USGS in the period 1950-2015. Data for the year 2020 was extrapolated using the best fit line from 2010 to 2015, and Q_p was assumed to be zero prior to 1950.

Finally, monthly recharge (R) in each basin was estimated from the watershed-scale parameters discussed above,

$$R = P - ET - Q_p$$

and mean R from the period of record in each basin was matched with the period of record mean Q_b.

Time Lag Estimation

Prior to using cross-correlation to determine Δt between R and Q_b, high frequencies in both the R and Q_b time series were filtered out using 11 different moving average windows from 10 to 20 years in length. The centered moving average windows were applied to the time series such that the beginning and end of each time series was truncated by half the length of the moving average window. For example, a 20 year moving average window results in a time series that begins 10 years later and ends 10 years earlier than the raw time series (Figure S1). Cross-correlation analysis was done on each of the 11 pairs of time series for each basin (one set of R and Q_b time series for each of the 11 moving average windows). The time increment that gave the highest correlation between R and Q_b was considered the Δt for each of the 11 sets of time series for each basin. Each basin was evaluated for the likelihood of having a long-term Δt between R and Q_b using the mean Δt (of the 11 estimated values for each basin) and the coefficient of variation (CV). Basins with mean $\Delta t <$ 1 were determined to not have a long term lag between R and Q_b, basins with mean $\Delta t >$ 1 but with

CV > 0.3 were determined as unlikely to have a long term lag between R and Q_b, and basins with mean Δt > 1 and with CV < 0.3 were determined as likely to have a long term lag between R and Q_b. For the 2 basins discussed in this document, only Basin 48 was determined as likely to have a long term lag between R and Q_b (Table S2). Thus, only Basin 48 has satisfied the first condition for basins showing evidence of FSI impacts to the water balance.

Table S2: Estimated Δt statistics for the 11 sets of R and Q_b time series between all 3 basins.

Basin	Mean Δt	Standard Deviation of Δt	CV of Δt
Basin 46 – Satilla River, GA	3.96	5.2	1.3
Basin 48 – Silver River, FL	18.8	0.70	0.037

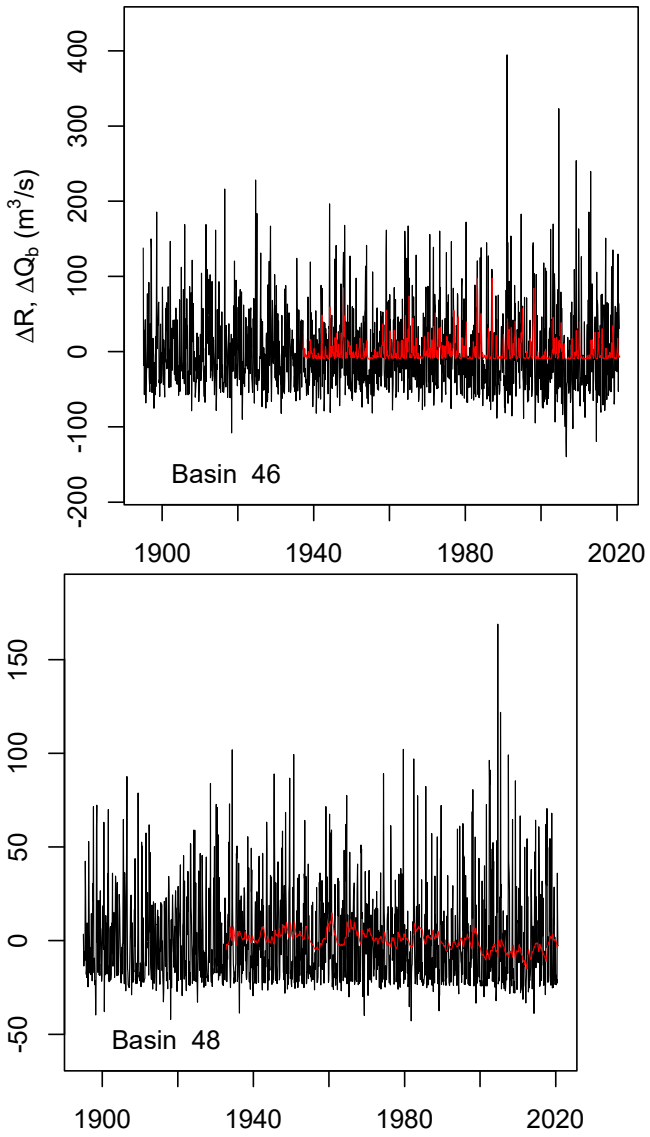
ΔR, ΔQb (m3/s)
400
300
200
100
0
-100
-200
Basin 46
1900
1940
1980
2020

150
100
50
0
-50
Basin 48
1900
1940
1980
2020

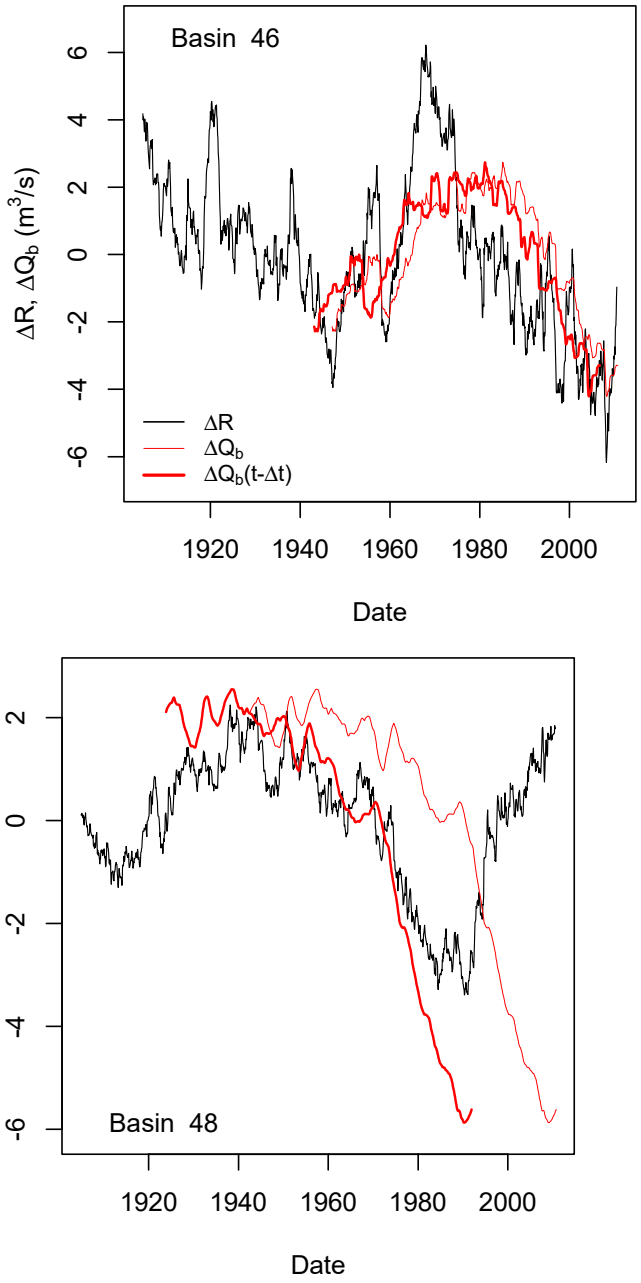

Figure S1: Time series of R (black) and Q_b (red) for each basin both prior to moving average window (top row) and after moving average window (bottom row). A moving average window of 20 years was used on the bottom row, and the lagged Q_b time series is shown in dark red. The period-of-record mean was subtracted from each time series before plotting.

Aquifer Storage Estimation

Time series of change in storage (ΔV) were estimated to determine the quantity of groundwater storage change relative to groundwater level fluctuations (Δh). The ΔV time series was determined as the cumulative difference between R and Q_b divided by A_{basin}

$$\Delta V = \frac{\sum_{t_0}^{t_n}\left(R(t_i) - Q_b(t_i)\right)}{A_{basin}}$$

where t_0 is the first time point in the time series and t_n is the final time point in the time series. Basins with $\frac{\Delta V}{\Delta h} > \eta$ were considered to have evidence of FSI impacts to the water balance. Both ΔV and Δh time series were averaged with a 10-year moving window and the long term mean was subtracted from both time series for each basin (Figure S2).

The storage coefficient S for each basin was estimated by maximizing the Nash-Sutcliffe efficiency (NSE) between ΔV and Δh. This estimation was performed in R using the *optimize* function which maximizes the target value (NSE in this case) by adjusting a specified variable (S in this case) between user-defined limits. The limits of S were set to (0,50). This methodology led to S = 0.17 in Basin 46 and S = 2.5 in Basin 48 (Table S3). For Basin 46, this value indicates that the change in storage is about 0.17 times the change in head in this basin, which meets expectations for unconfined aquifers that are not impacted by the FSI. For Basin 48, the estimated S value suggests the change in storage is about 2.5 times the change in head. The FSI provides the storage mechanism necessary to reach this value of S in Basin 48 by moving approximately 40 times the distance that the potentiometric surface moves. Thus, the value of S in Basin 48 suggests evidence of FSI impacts, and Basin 48 meets the second condition needed for basins showing FSI impacts on the water balance.

Table S3: Estimated values of S for each basin along with the resulting NSE between the best fit Δh time series and the ΔV time series.

Basin	S	NSE	FSI impacts
Basin 46 – Satilla River, GA	0.171	0.84	No
Basin 48 – Silver River, FL	2.46	0.80	Yes

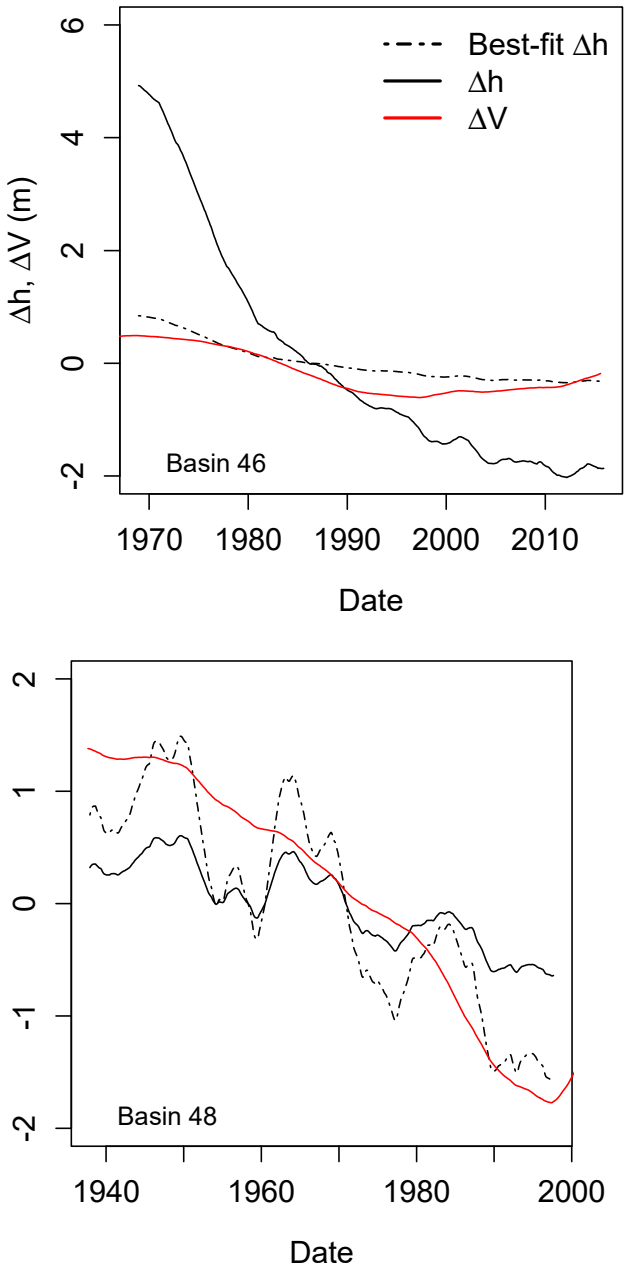

Figure S2: Time series of ΔV (red) and Δh (black) with best fit Δh plotted as a dotted black line for the two basins. The solid black line multiplied by S gives the dotted black line. NSE was estimated between the best fit Δh time series and the ΔV time series.

FSI Impact Conclusion

Detailed analysis for two of the 68 basins used in this study was given in this document. The conditions for FSI impacts to the water balance were defined as 1) Δt > 1 year with CV < 0.3 and 2) $S > \eta$. The maximum value for η was discussed in the main text as 0.4. Basin 46 (Satilla River, GA)

did not satisfy either condition for FSI impacts, while Basin 48 (Silver River, FL) satisfied both conditions for FSI impacts. Thus, Basin 48 was considered to have significant evidence of FSI impacts to the water balance. If one of these basins had satisfied only one of the defined conditions for FSI impacts, then that basin would have been determined as unlikely to be impacted by the FSI. Because Basin 46 satisfied neither condition, this basin was also determined as unlikely to be impacted by the FSI.

References

32. Nathan, R.; McMahon, T. Evaluation of automated techniques for baseflow and recession analyses. *Water Resour. Res.* **1990**, *26*, 1465–1473.
33. PRISM Climate Group, Oregon State University, 2021. Available online: https://prism.oregonstate.edu (accessed on 12 January 2021).
34. Lu, J.; Sun, G.; McNulty, S.; Amatya, D. A comparison of six potential evapotranspiration methods for regional use in the southeastern United States. *J. Am. Water Resour. Assoc.* **2005**, *41*, 621–633.
35. Hargreaves, G.; Samani, Z. Estimating potential evapotranspiration. *J. Irrig. Drain. Div.-ASCE* **1982**, *108*, 225–230.
36. Samani, Z. Estimating solar radiation and evapotranspiration using minimum climatological data. *J. Irrig. Drain. Eng.* **2000**, *126*, 265–267.
37. Allen, R.G.; Pereira, L.S.; Raes, D.; Smith, M. *Crop Evapotranspiration—Guidelines for Computing Crop Water Requirements*; FAO Irrigation and Drainage Paper, 56; FAO: Rome, Italy, 1998.
38. Choudhury, B. Evaluation of an empirical equation for annual evaporation using field observations and results from a biophysical model. *J. Hydrol.* **1999**, *216*, 99–110.
55. Gubler, S.; Hunziker, S.; Begert, M.; Croci-Maspoli, M.; Konzelmann, T.; Bronnimann, S.; Schwierz, C.; Oria, C.; Rosas, G. The influence of station density on climate data homogenization. *Int. J. Climatol.* **2017**, *37*, 4670-4683.